Sort of summary of the work done from January through August 2000

Milena Veneziani, August 9^{th}

1 Introduction

The study of the ocean by the Lagrangian point of view allows two different kinds of applications. A "direct" approach involves studies of the tracer trajectories; the dispersion of ensambles of particles are usually analyzed together with the trasport and mixing related to it. On the other hand, the "inverse" problem can be adressed of extracting information about the velocity field and the circulation from a Lagrangian data set (either real or numerical simulated).

In the framework of the first approach, a possible application is studying the dispersion of fish larvae, preferably of those species whose biological behavior, at their first stage, has already been investigated. This is the case for snapper larvae spawning in several Carribean sites, whereas still little is known about the grunt larvae biology and spawning events. Lindeman et al. (1999???) have investigated the possible transport scenario of these two larvae species in the region southwest of Cuba, in the Yucatan Channel and in the lower Florida Keys. The common belief about the transport features in the northern Caribbean is a strong unidirectional flow which advects the particles into the Yucatan Channel and then away from the region, through the Florida Current. Based on lagrangian drifters data and on current mooring data, the work by Lindeman et al. suggests instead that there is evidence of partial retention southwest of Cuba, in the eastern Yucatan Channel and in the Tortugas Gyre, slightly north of the lower Florida Keys.

The next step in this investigation involves the numerical modelling of the lagrangian trajectories and the comparison with the real data and the preceding biological results. This work has concerned the simulation of passive tracers trajectories, by integrating the velocity field generated by the ocean general circulation model Miami Isopycnal Coordinate Ocean Model (MICOM). A cloud of 1000 particles has been released at three different sites, for two families of snapper larvae and the evolution has been tracked for 40 days, representing the typical Planktonic Larval Duration of these species (the mean is 32 days). The characteristics of the deployments and the releasing times are showed in Table **??**. The real larvae experience a dayly vertical migration of 50 meters, but the snappers still remain in the mixed layer; for this reason, we chose to integrate the modelled surface velocity which is representive of the depth-averaged mixed layer.

Release site	Species	Release time
SW of Cuba		
($\phi = 21°27'N$, $\lambda = 82°13'W$)	Mutton Snapper	May 30^{th}
	Gray Snapper	July 15^{th}
Florida Keys		
($\phi = 24°29'N$, $\lambda = 83°07'W$)	Mutton Snapper	May 30^{th}
	Gray Snapper	Aug. 15^{th}
Yucatan Channel		
($\phi = 18°23'N$, $\lambda = 87°22'50''W$)	Mutton Snapper	May 30^{th}
($\phi = 18°33'N$, $\lambda = 87°18'W$)	Gray Snapper	July 15^{th}

Table 1: Coordinates of the deployment and releasing times for the two snapper species analyzed.

The code used to simulate the trajectories is described in section 1, together with the lagrangian stochastic model introduced to simulate the sub-grid scale motions that are not resolved by MICOM. Finally, the results are presented in section 3 and the limits of the experiments are discussed, along with the possible future improvements of the model.

2 Description of the model

The dayly MICOM velocity field, which is distributed on a Arakawa C-grid, is integrated using a second order Runge-Kutta method; any data which need to be available at a shorter time step than one day, must be interpolated in time (linear interpolation so far).

The deterministic large scale flow has spatial and temporal scales directly tied to the resolution of the model and related to the time variability of the forcing which is represented, in this case, by the COADS monthly climatological winds. At the MICOM field U we add a random velocity component u' representing the sub-grid scale features and the highly time variable structures that are filtered out by the climatological forcing of the model. This aim is accomplished by applying a stochastic particle model (see e.g. Thomson 1987, Griffa 1996) under the assumptions that the velocity random process is:

1. stationary in time, at least up to the second order, which means that the velocity mean $< u' >$ and variance $< u'^2 >$ are constant in time and the autocorrelation function depends only on the time lag between two different values of velocity;

2. homogeneous, with similar properties concerning the spatial dependence;

3. isotropic, which is not an essential condition and it is made just to semplify the problem since the cross-covariance $< u'v' >$ drops off in the equations;

4. in absence of any coherent flow structures which would introduce a stronger dependence of the random velocity at the actual time on the values at different preceding times.

Domande Annalisa....:

—> il fatto che $< u' >= 0$ da che dipende esattamente? dal particolare Lagrangian model

oppure no? a me sembrerebbe che $< u' >= 0$ piu' nel modello 0...
—> che cosa succede all'autocovarianza quando il processo e' non stazionario??? e quindi come cambia tutto il resto che e' legato all'autocovarianza (dispersione, K,...)??
—> credo che il comportamento di K per $t << Tlag$ (balistic?) dipenda dalla particolare autocorrelazione e quindi dall'ordine del LSM, mentre per $t >> Tlagr$ no, vero?
—> vorrei cercare di capire come legare il K dei vari LSM col K eddy diffusivity coefficient nelle momentum equations...

The last assumption allows us to consider the stochastic velocity as a Markovian process for which the field at time t_n depends only on the value at t_{n-1}. In particular, according to the "randomness" of either the position process $x(t)$ or the velocity $u'(x,t)$ or the acceleration du'/dt, the lagrangian models of different order provide increasingly detailed descriptions of particle motion.

The first order model assumes that x is Markovian whereas the velocity field is completely random and independent from any preceding values. On the other hand, the second order model has x and u' jointly Markovian, so that the random velocity is correlated with the preceding value up to a time T_L which is called *Lagrangian time scale*. This model is a better rapresentation of the real fluid motion that has a certain "memory" based on its initial conditions. Finally, an even more realistic model has also the actual acceleration depending on its preceding value and a further correlation time scale is introduced.

In the simulation of the larvae dispersion we applied the second model, since it has been proven (e.g. Griffa et al. 1995, Krauss and Boning 1987) to be a good enough rapresentation for surface turbolent flows, especially in restricted areas where the stationarity and homogeneity assumptions still remain valid.

The incremental equations which describe the particle motion due to both the deterministic and the random flow are:

$$dx = Udt + u'dt \tag{1}$$

$$du' = -\frac{u'}{T_L}dt + \sqrt{\hat{K}}dw \tag{2}$$

where some variables have already been defined above, dw is a random increment from a normal distribution and $\hat{K}$ is proportional to the eddy diffusivity coefficient K and is given by:

$$\hat{K} = \frac{< u'^2 >}{T_L} = \frac{K}{{T_L}^2}$$

The equation **??** is known as *Langevin equation* (e.g. Taylor 1921, Csanady 1980).

Our next step has concerned the choice of the parameters T_L and $\hat{K}$ (where $\hat{K}$ is tied to the variance $< u'^2 >$). The Lagrangian time scale for the ocean surface lies in the range 1-4 days, so we made the reasonable choice of 2 days. Picking up a value for the eddy diffusion is a bit more delicate problem because $\hat{K}$ is somehow representive of the sub-grid spatial and temporal structures that are not solved by MICOM. Moreover, the variance $< u'^2 >$ is strongly tied to the eddy kinetic energy of the region in question, whereas we need to keep the process homogeneous.

A first value for $\hat{K}$ has been obtained by using the bulk MICOM eddy diffusivity coefficient, which is $K \sim 10^6 cm^2/s$ (true?), in order to introduce back the sub-grid scales. Led by the awareness that the real motion is even more turbolent because of the smooth MICOM forcing, the next experiment has been carried out with $K = 10^7 cm^2/s$, which will be the upper limit for a reasonable simulation. This last value of K has been deducted by the comparison between the MICOM simulated trajectories and the *in situ* drifter data carried out by Garraffo et al. (2000a).

In section 3 we present first the experiment with no turbulent velocity field ($K = 0$) and then those with $K = 1.7 \times 10^6 cm^2/s$ and $K = 10^7 cm^2/s$ respectively.

3 Results

The work will be presented in terms of snap-shop figures at intervals of 10 days and some trajectories plots for the three sites, southwest of Cuba, the Florida Keys and the Yucatan Channel, and for the two snapper species. The particles representing the Mutton larvae are released on May 30^{th} which is the middle of the spawning season, whereas the Gray snappers are relative to a later summer period, ranging between July and August 15^{th}. The figures **??** and **??** show the simulations in the region close to the Cuban coasts; from them we definitely recognize a retention behavior for all the experiments. After 30 days, most of the larvae stay within 300 km from the shelf and the particles are not advected by the strong current flowing through the Yucatan Channel. The figures **??** and **??** show some of the trajectories. We notice a rather similar behavior for the two larvae species.

The scenario changes when we consider the site close to the lower Florida Keys; the figure **??**, which describes the dispersion of Mutton larvae, points out that most of the particles are advected by the Florida current and a few of them spreads up to the north. A completely different situation arises from fig. **??** representing the evolution of Gray larvae; indeed in this case the retention behavior is predominant due to a migration of the Florida current front towards the south and the trapping of the particles within the Tortugas Gyre. Again, the figures **??** and **??** show some of the trajectories simulated in this region.

Finally, we consider the dispersion simulation in the Yucatan Channel; from fig. **??** through **??** we notice that no retention is experienced. This is expectable since the releasing site is located right inside the strong Yucatan flow and the particles are easily advected by the loop current in the Gulf of Mexico and later by the Florida current.

In conclusion we should mention that in some of the regions taken in consideration, the assumption of homogeneous and stationary turbulence does not exactly hold. The intense shears and the associated instabilities close to the western boundary currents generate intensifications of the turbulent activities which should be taken in account. Moreover, in coastal regions the turbulent parameters depend on the distance from the coast. For these reasons a natural development of the numerical simulations showed here, would involve non-homogeneous lagrangian stochastic particle models, especially in highly energetic and coastal areas.

References

[1] Csanady, G. T., 1980. *Turbulent diffusion in the environment*. Dordrecht, D. Reidel Publ. Co., 248 pp.

[2] Garraffo, Z. D., A. J. Mariano, A. Griffa, C. Veneziani and E. Chassignet, 2000a. Lagrangian data in a high resolution numerical simulation of the North Atlantic. I: Comparison with *in-situ* drifter data. *J. Mar. Systems*, accepted.

[3] Griffa, A., 1996. The use of stochastic particle models in oceanography. In *Stochastic modelling in Physical Oceanography*, Eds. R. Adler, P. Muller and B. Rozovskii, Birkhauser.

[4] Griffa, A., K. Owens, L. Piterbarg and B. Rozoskii, 1995. Estimates of turbulence parameters from Lagrangian data using a Stochastic Particle Model. *J. Mar. Res.*, **53**, 371-401.

[5] Krauss, W. and C. W. Boning, 1987. Lagrangian properties of eddy fields in the northern Atlantic as deduced from satellite-tracked buoys. *J. Mar. Res.*, **45**, 259-291.

[6] Lindeman, K. C., T. N. Lee, W. D. Wilson, R. Claro and J. S. Ault, 1999?. Transport of larvae originating in southwest Cuba and the Dry Tortugas: evidence of partial retention in Grunts and Snappers. *Proc. Gulf Carib. Fisheries Inst.*, **52**,...

[7] Taylor, G. I., 1921. Diffusion by continuous movements. *Proc. Lond. Math. Soc.*, **20**, 196-212.

[8] Thomson, D. J., 1987. Criteria for the selection of stochastic models of particle trajectories in turbulent flows. *J. Fluid Mech.*, **180**, 529-556.

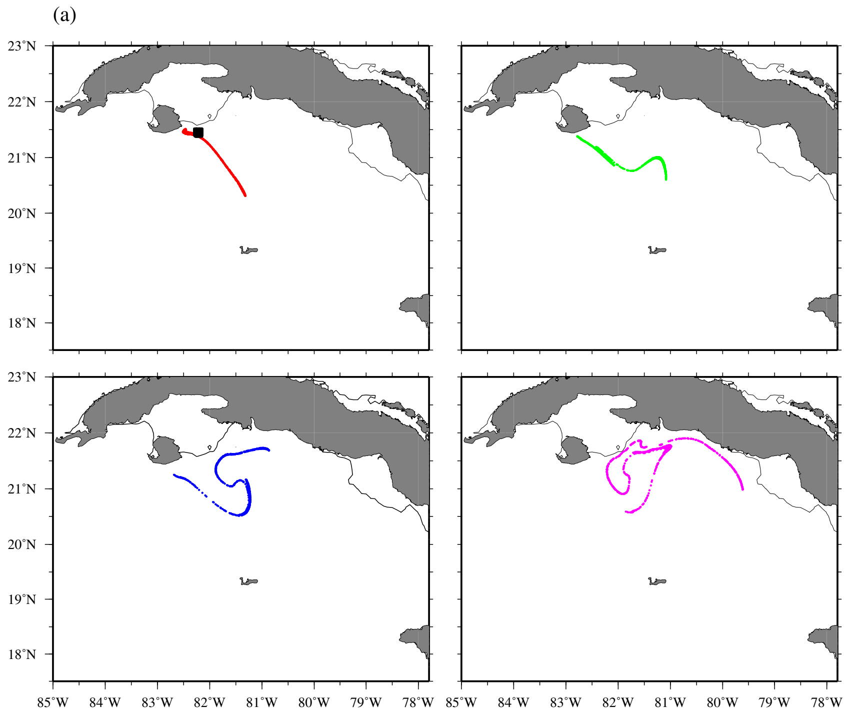

Figure 1: Mutton snapper larvae dispersion southwest coasts of Cuba with no turbulent velocity (a), with an eddy diffusion of $K = 1.7 \times 10^6 cm^2/s$ (b) and with $K = 10^7 cm^2/s$ (c). The black dot represents the deployment site; the red dots are the positions of the 1000 particles after 10 days; green, blue and magenta after 20, 30 and 40 days, respectively. The bathymetry profile is relative to the 30 m depth.

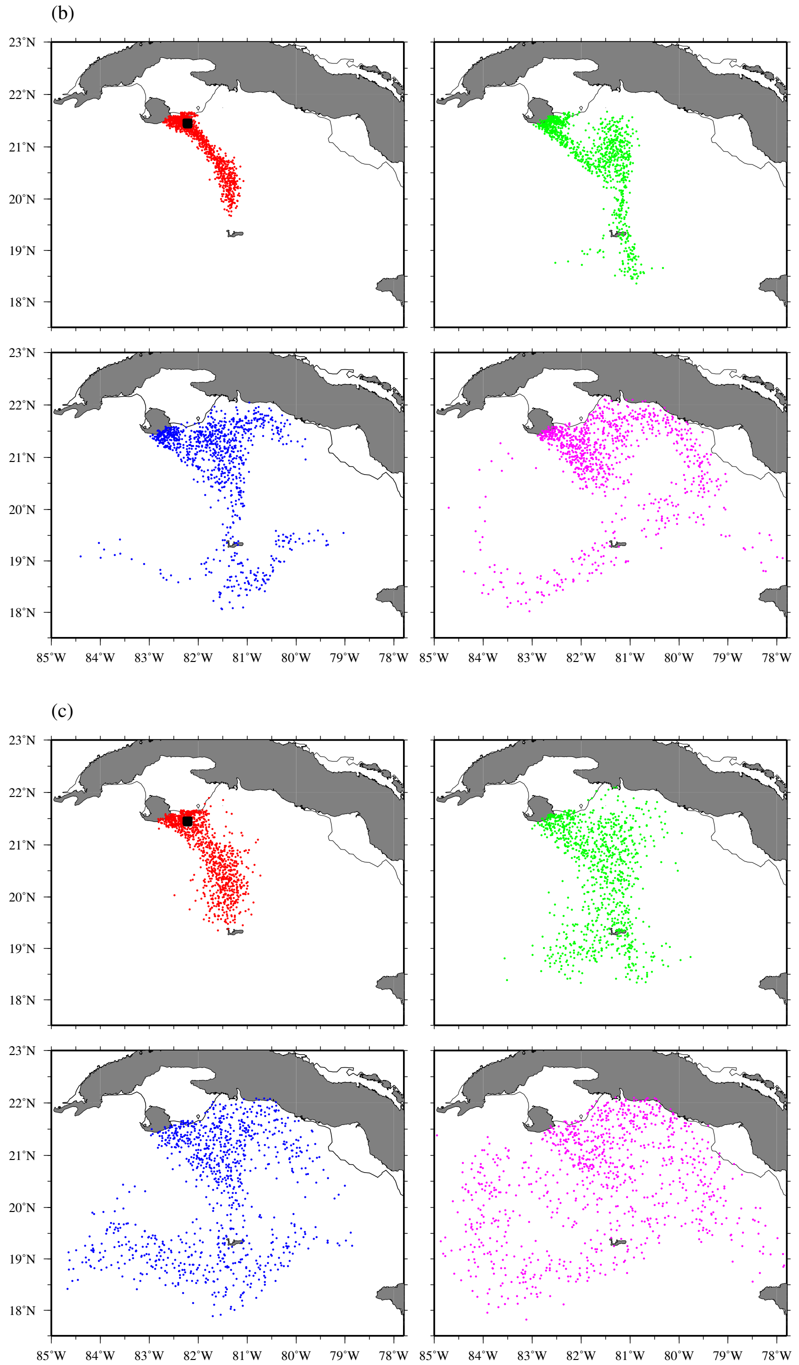

Figure 1: Cont'd.

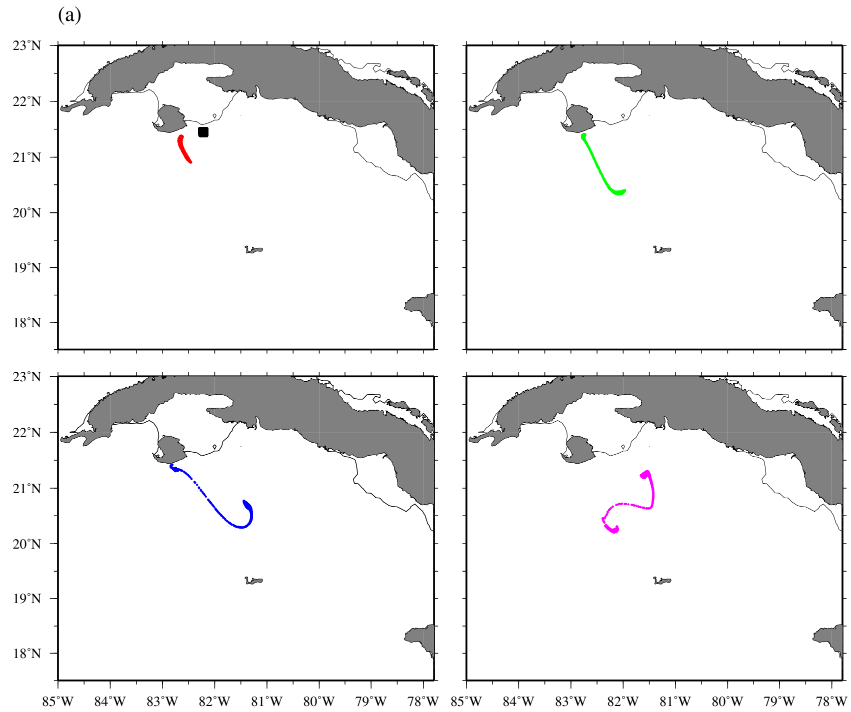

Figure 2: Gray snapper larvae dispersion with the same features as in fig. **??**.

(b)

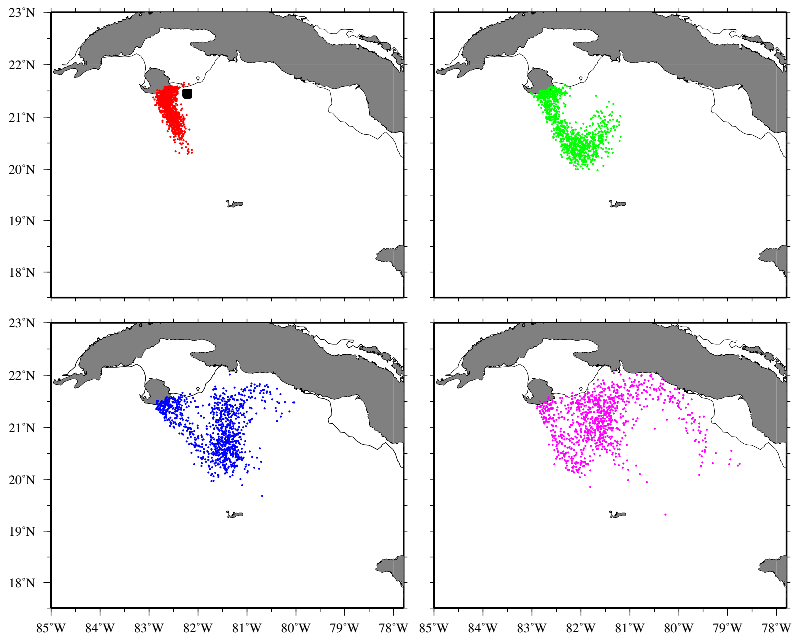

(c)

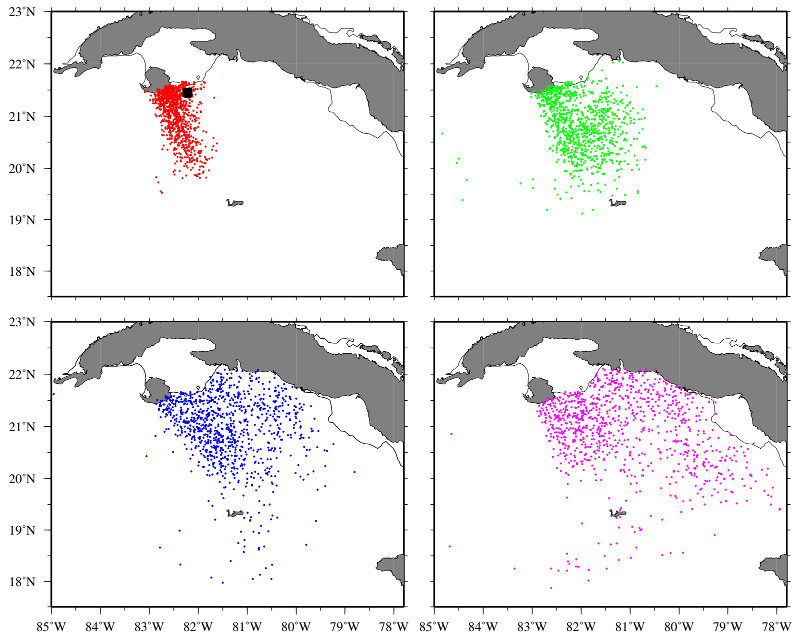

Figure 2: Cont'd.

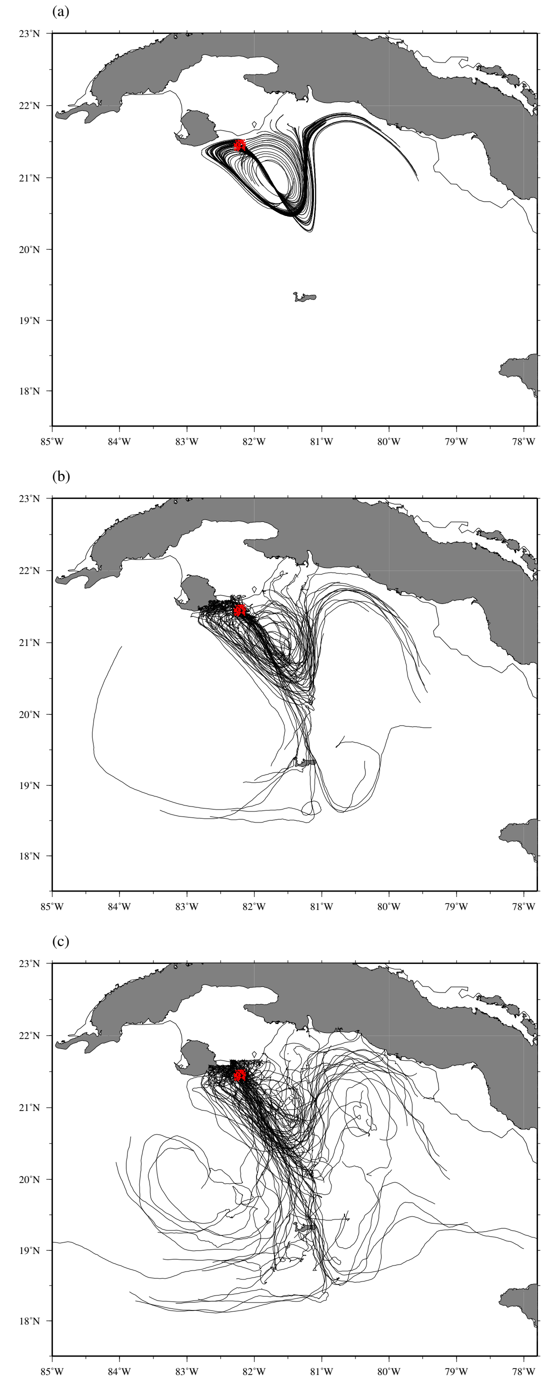

Figure 3: A sample of 80 trajectories for the Mutton larvae case and for the three different eddy diffusions (a,b,c, respectively). The red dots are the initial positions.

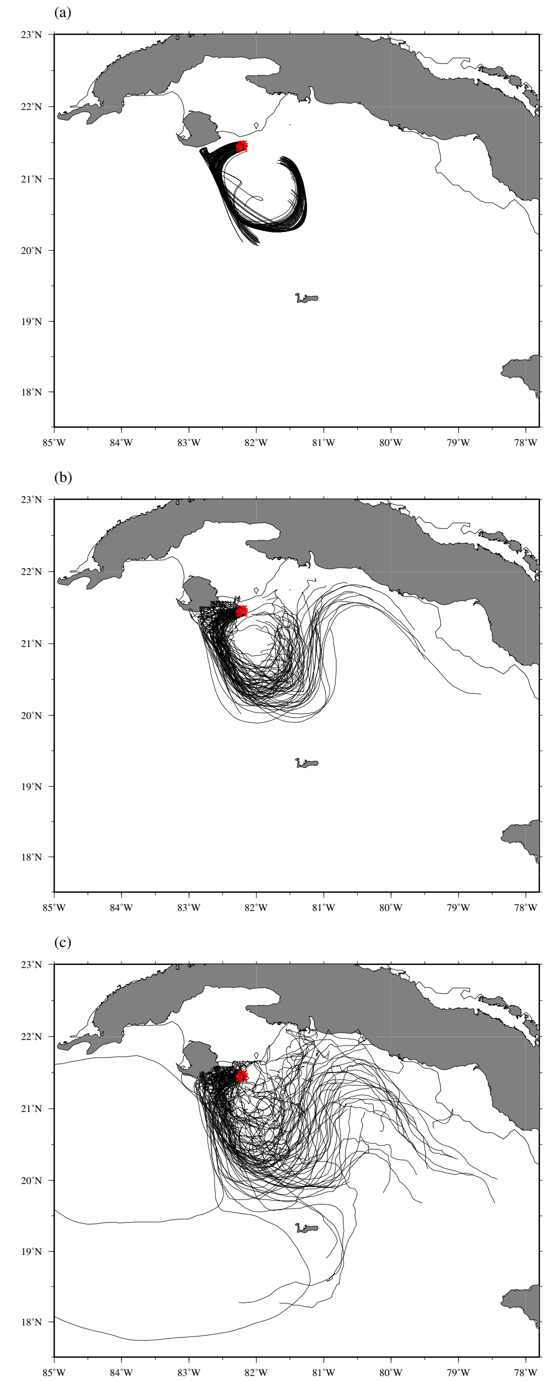

Figure 4: Same as fig. **??** but for Gray larvae.

a)

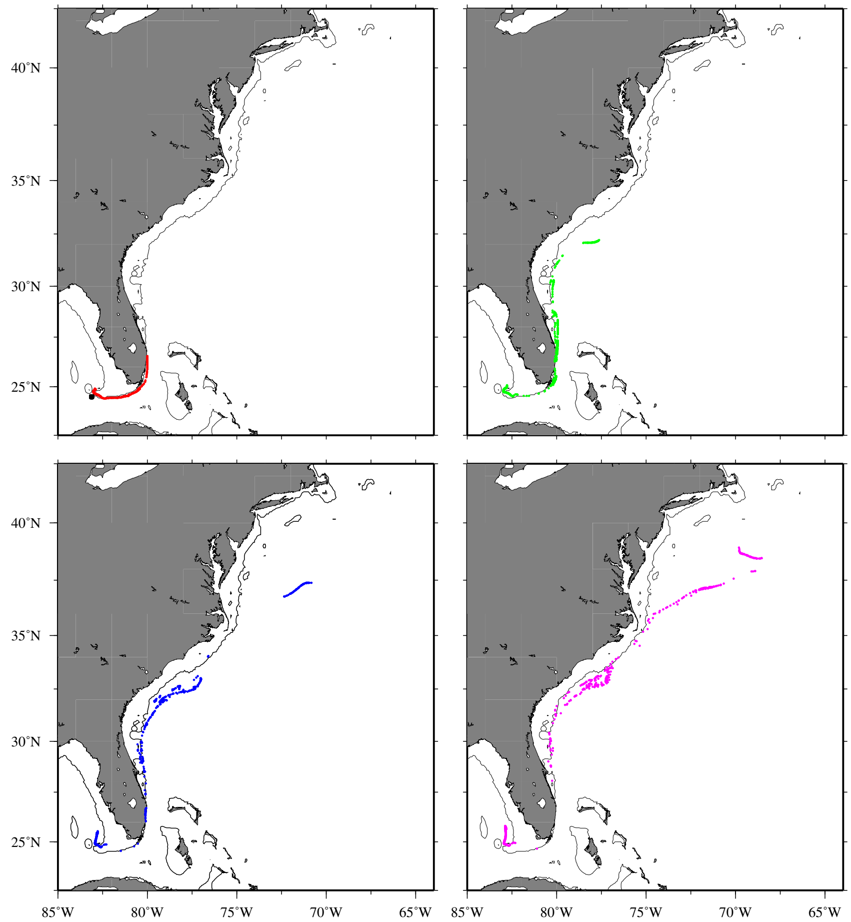

Figure 5: Same as in fig. **??** but for the lower Florida Keys region.

b)

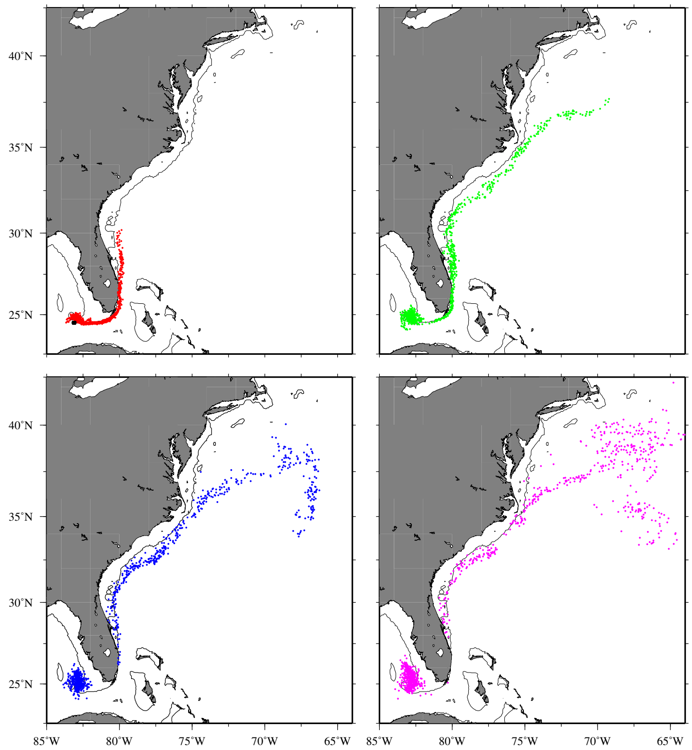

c)

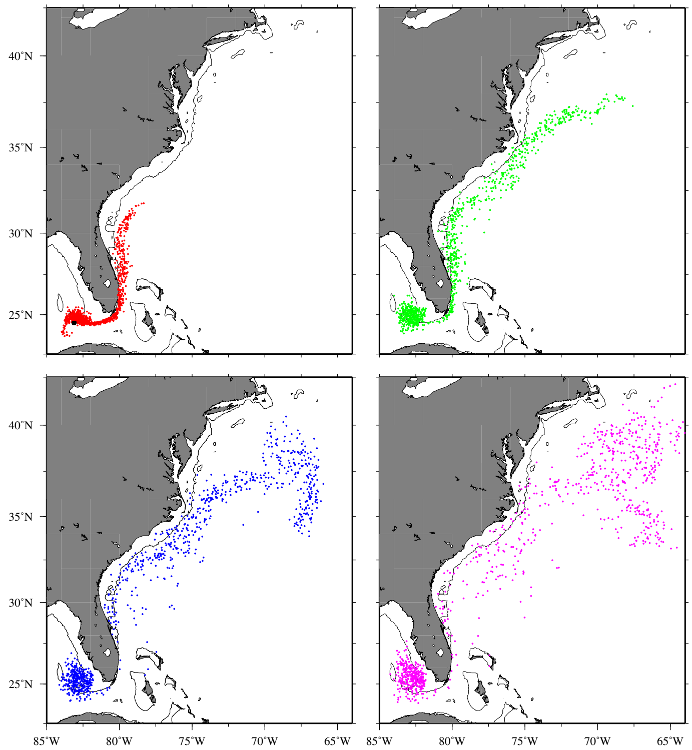

Figure 5: Cont'd.

a)

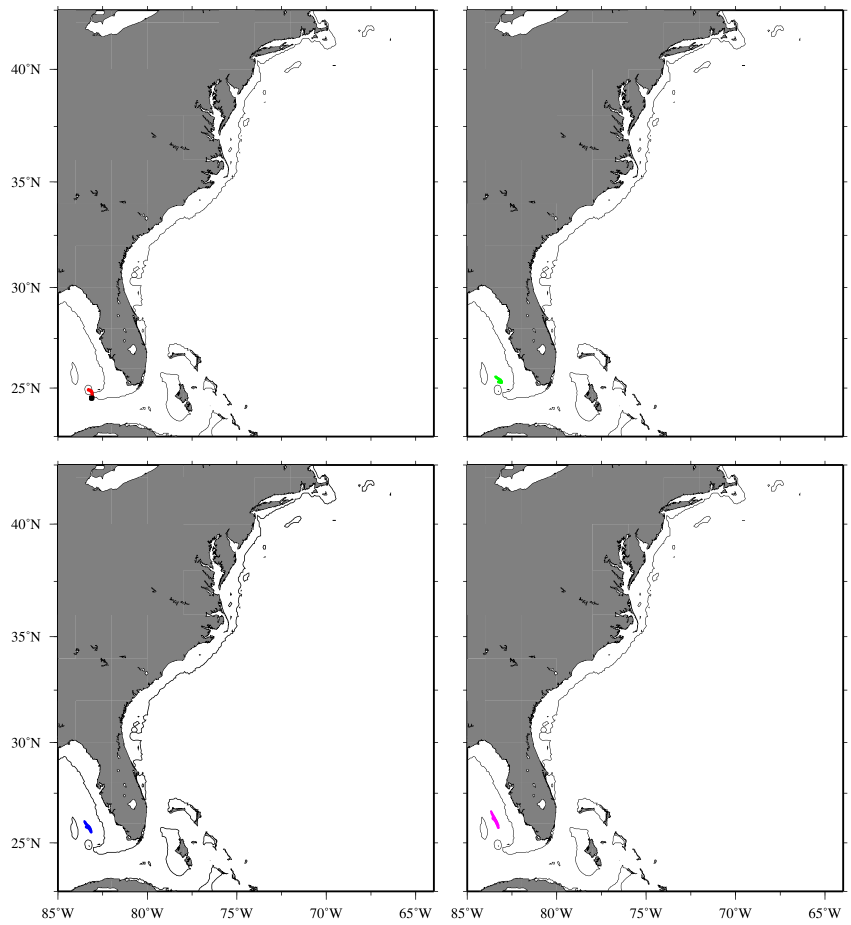

Figure 6: Gray snapper larvae dispersion with the same features as in fig. **??**.

b)

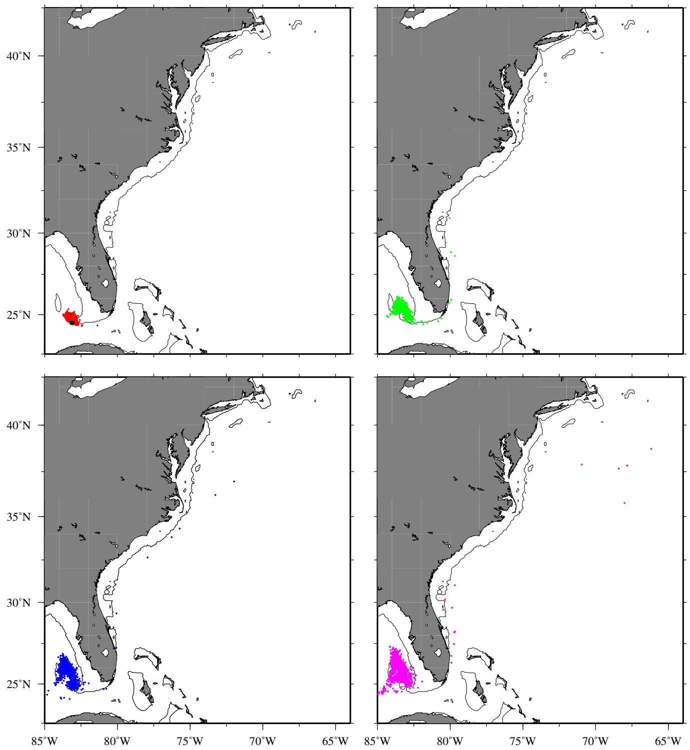

c)

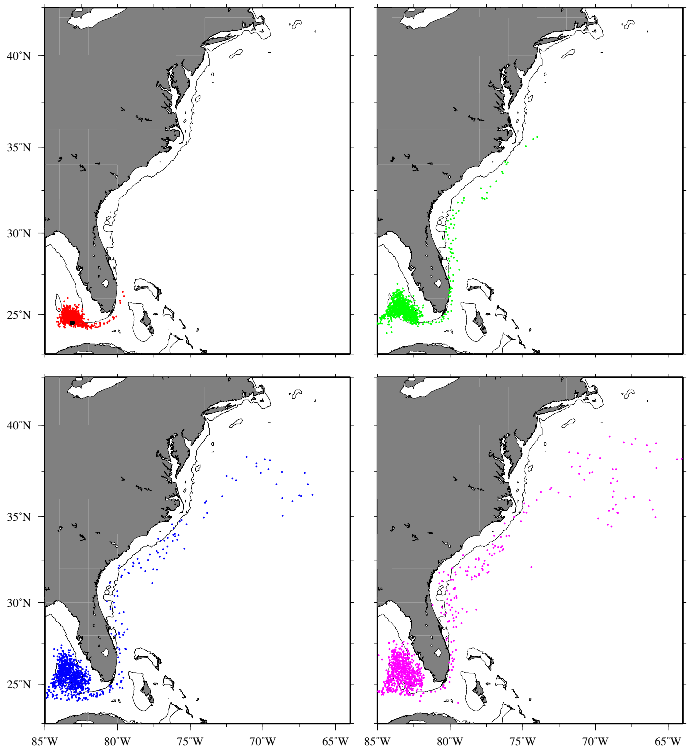

Figure 6: Cont'd.

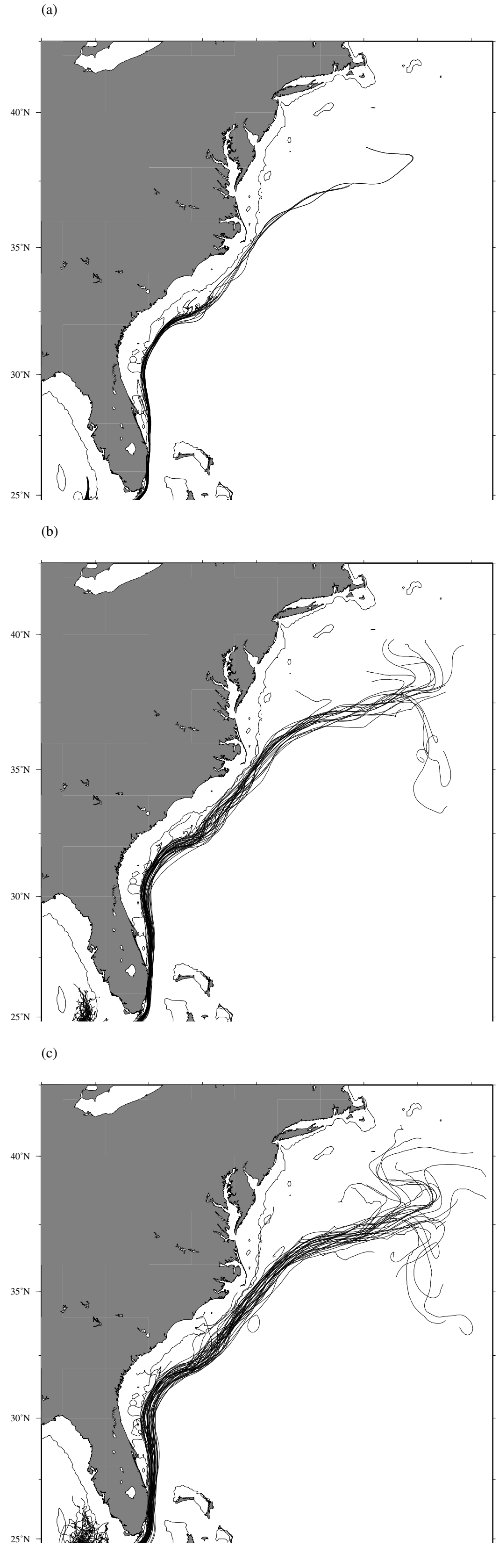

Figure 7: Same as fig. **??**.

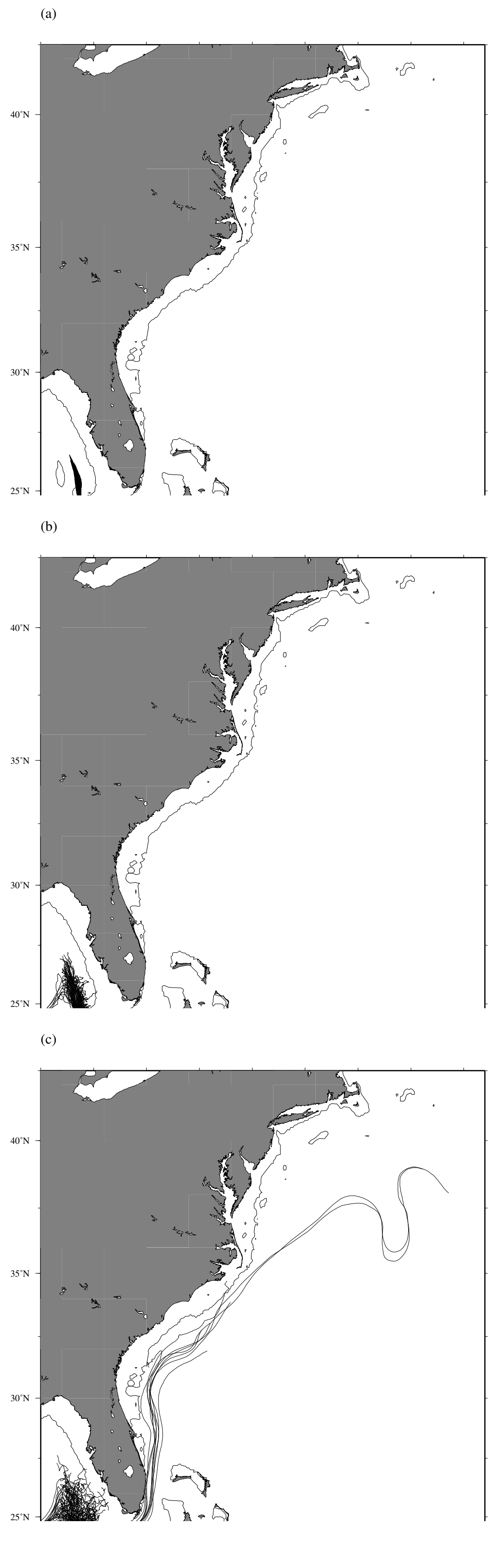

Figure 8: Same as fig. **??**.

a)

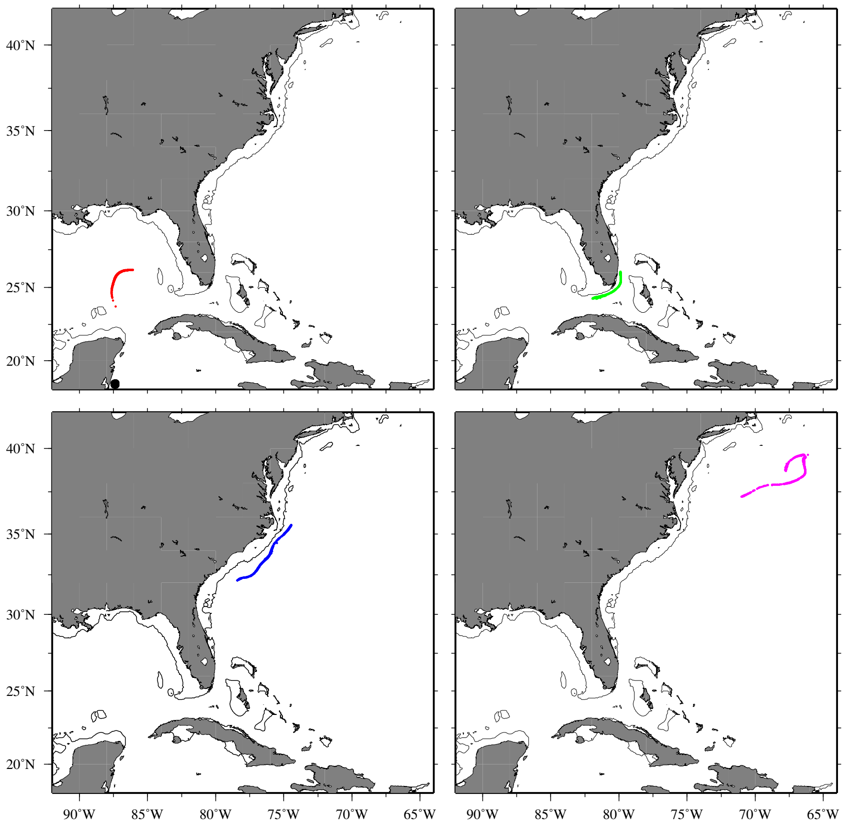

Figure 9: Same as in fig. **??** but for the Yucatan channel region.

b)

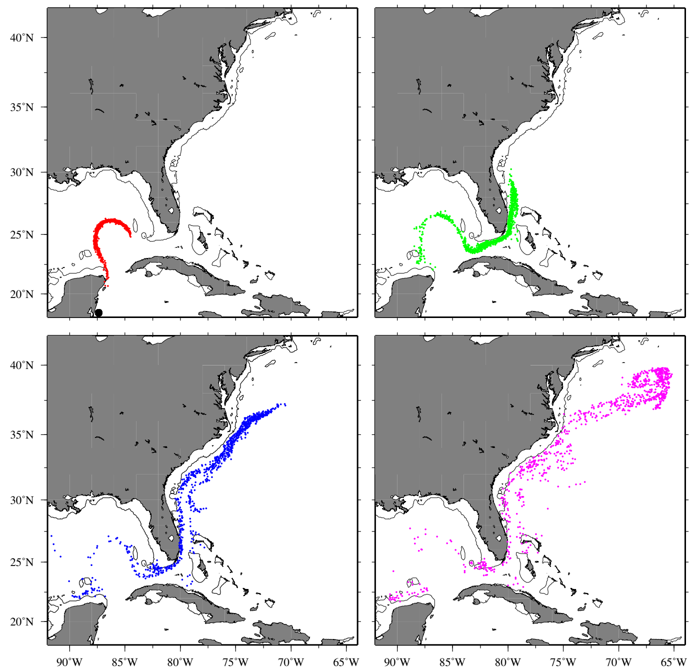

c)

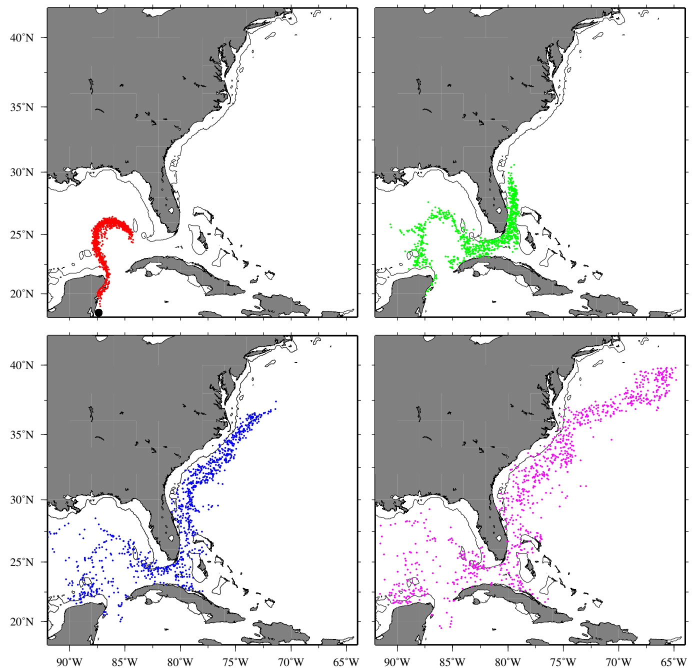

Figure 9: Cont'd.

a)

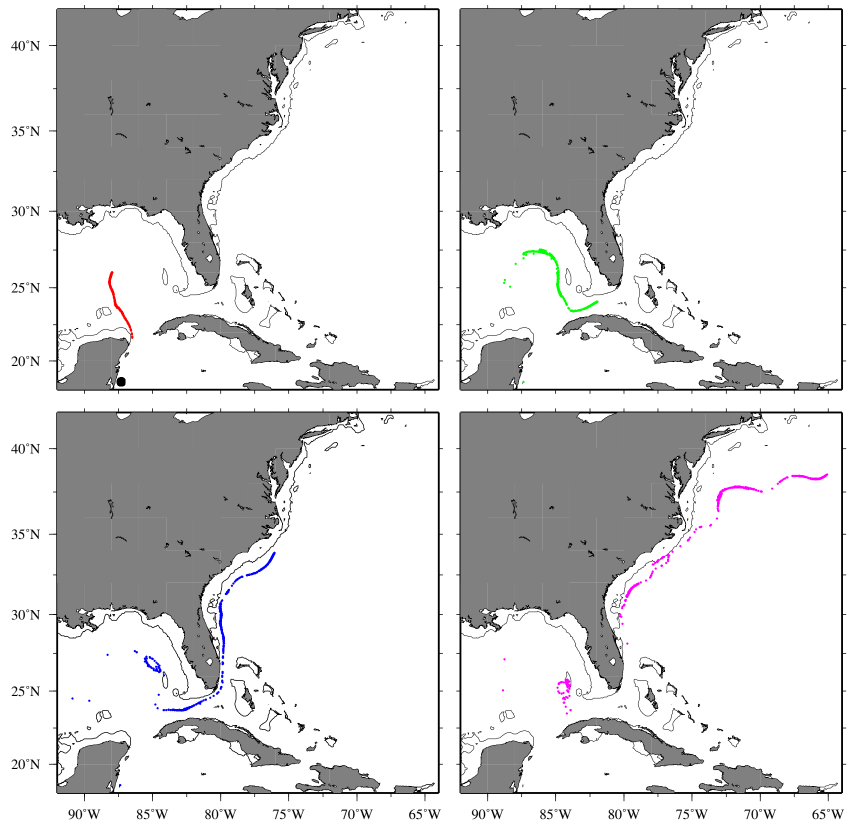

Figure 10: Gray snapper larvae dispersion with the same features as in fig. **??**.

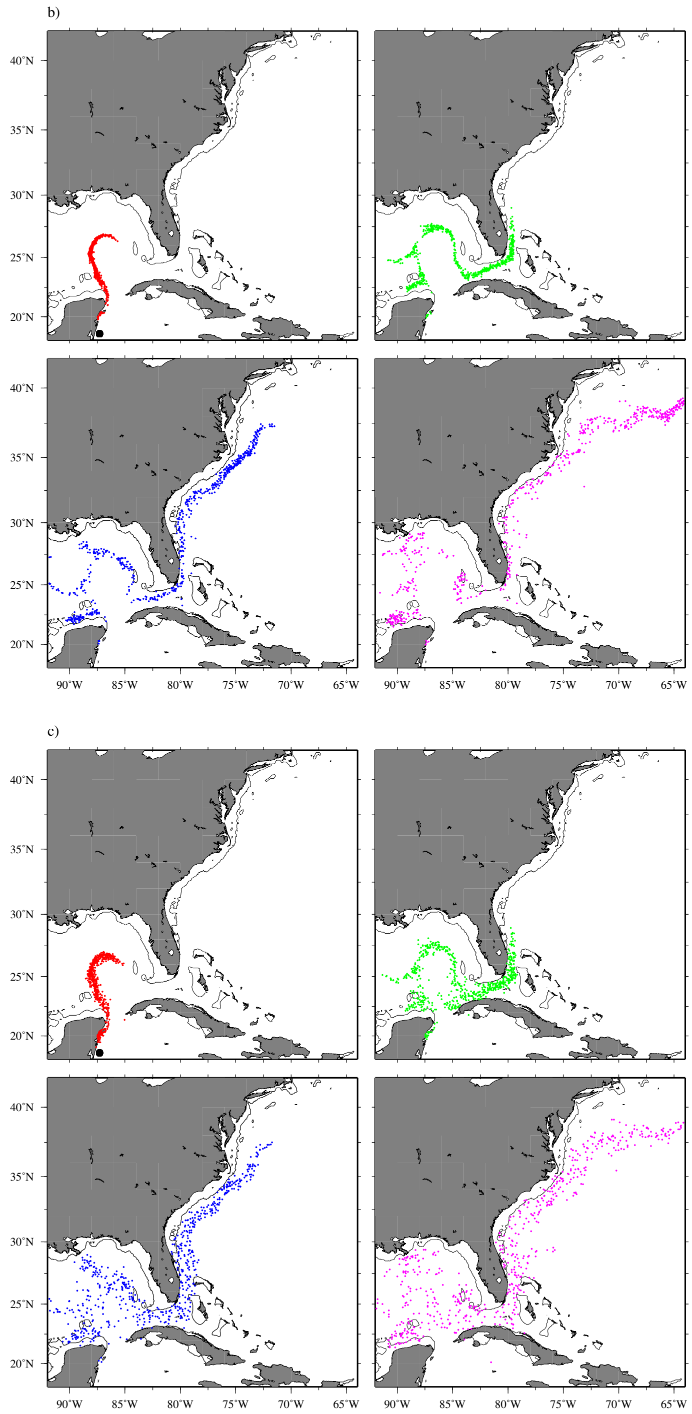

Figure 10: Cont'd.

(a)

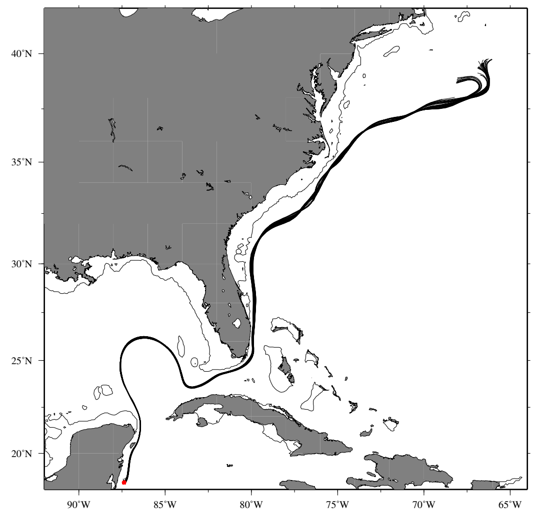
40°N
35°N
30°N
25°N
20°N
90°W
85°W
80°W
75°W
70°W
65°W

(b)

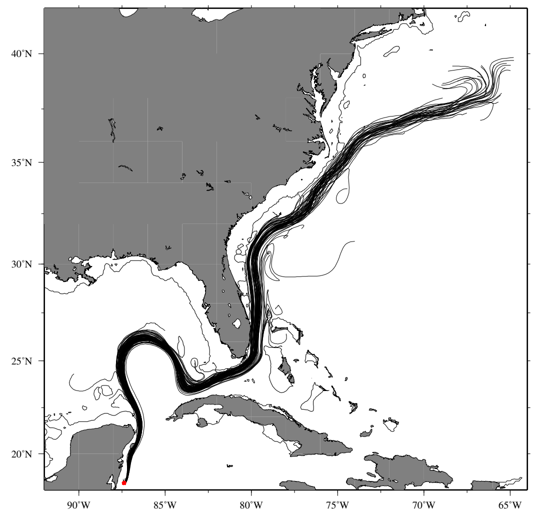
40°N
35°N
30°N
25°N
20°N
90°W
85°W
80°W
75°W
70°W
65°W

(c)

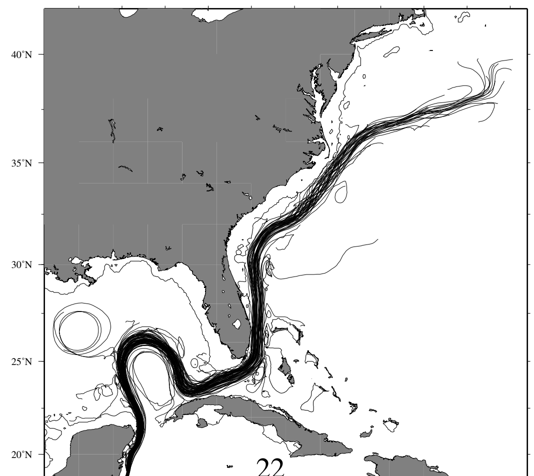
40°N
35°N
30°N
25°N
20°N

(a)

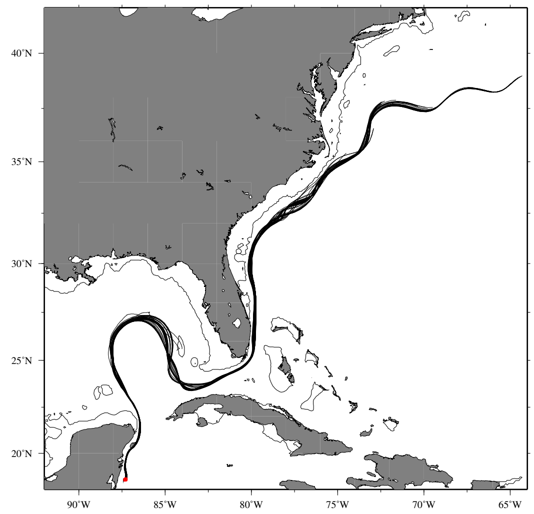
40°N
35°N
30°N
25°N
20°N
90°W
85°W
80°W
75°W
70°W
65°W

(b)

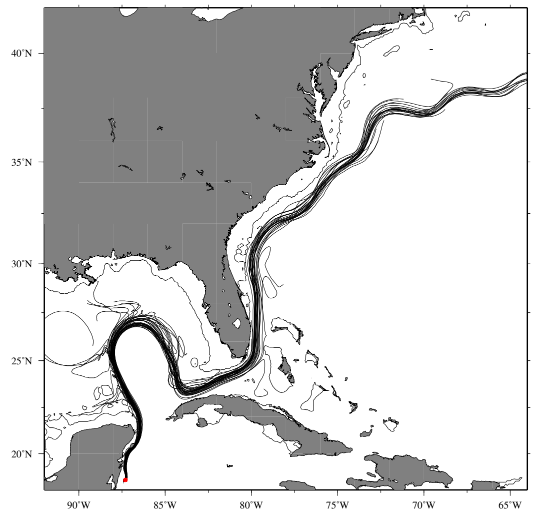
40°N
35°N
30°N
25°N
20°N
90°W
85°W
80°W
75°W
70°W
65°W

(c)

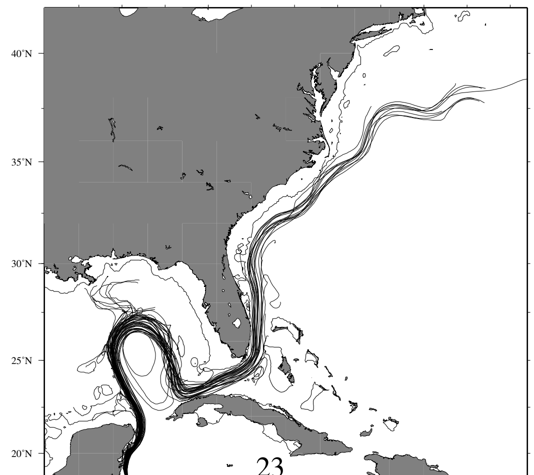
40°N
35°N
30°N
25°N
20°N